Two New Mixed-Valence Manganese Complexes of Formula $[Mn_4O_2(X\text{-benzoato})_7(bpy)_2]$ (X = 2-Cl, 2-Br) and the Crystal Structure of the 2-Cl Complex: Ground-State Spin Variability in the $[Mn_4O_2]^{7+}$ Complexes

Belen Albela, Mohamed Salah El Fallah, and Joan Ribas*

Departament de Química Inorgànica, Universitat de Barcelona, Diagonal, 647, 08028 Barcelona, Spain

Kirsten Folting and George Christou

Department of Chemistry, Indiana University, Bloomington, Indiana 47405-4001

David N. Hendrickson

Department of Chemistry, University of California—San Diego, La Jolla, California 92093-0358

Received September 19, 2000

The reaction of $[Mn_3O(2\text{-X-benzoato})_6L_3]$ (X = Cl, Br; L = pyridine) with 2,2′-bipyridine in CH_2Cl_2 leads to the high-yield formation of new mixed-valence tetranuclear $Mn^{II}Mn_3^{III}$ complexes of general formulation $[Mn_4O_2(X\text{-benzoato})_7(bpy)_2]$ (**1**, X = 2-chloro; **2**, X = 2-bromo). The crystal structure of **1** was determined. Complex **1** crystallizes in the monoclinic system, space group $P2_1/n$ with $a = 19.849(8)$ Å, $b = 13.908(5)$ Å, $c = 30.722(19)$ Å, $\beta = 107.35(2)°$, $Z = 4$. Complex **1** is neutral, and consideration of overall charge necessitates a mixed-valence $Mn^{II}Mn^{III}_3$ description. Each manganese ion is distorted octahedral, especially the three Mn^{III} ions, owing to a first-order Jahn−Teller effect. The Mn^{II} is assigned on the basis of the longer metal−ligand distances. Variable temperature magnetic susceptibility studies were performed on **1** and **2** in the temperature range 2−300 K. The topology of the molecule requires three *J* values, J_{bb} between the two-body Mn^{III} ions and two J_{wb} ("wing-body") between the Mn^{III} ions of the "body" of the butterfly and the Mn^{II} or Mn^{III} of the "wing" of the butterfly. Without any simplifying assumptions, a full diagonalization matrix method is necessary to solve the problem, but assuming that both J_{wb} are identical, it is then possible to solve the problem numerically by applying the Kambe method. With both methods, the derived J_{bb} and J_{wb} exchange parameters are very similar for the 2-Cl and 2-Br complexes. The best *R* factors $[\sum_i(\chi_{Mcalc} - \chi_{Mobs})^2/\sum_i(\chi_{Mobs})^2]$ ($\sim 10^{-6}$) were obtained from 300 to 40 K. The *J* values are, thus, as follows. For **1**, $J_{bb} = -23.2$ cm^{-1}, $J_{wb} = -4.9$ and -4.8 cm^{-1}, and $g = 1.93$. For **2**, $J_{bb} = -22.8$ cm^{-1}, $J_{wb} = -4.8$ and -4.7 cm^{-1}, and $g = 1.92$. With these values, the expected ground-state spin must be $^7/_2$, very close in energy to low-lying spin states of $^9/_2$, $^5/_2$, $^3/_2$, and $^1/_2$. They are all almost degenerate. By application of Kambe's method (with only one J_{wb}), the results are completely similar. Magnetization measurements at 2−30 K from 2 to 50 kG confirm that the ground state is $S = ^7/_2$ for **1**, with the *D* parameter equal to -0.60 cm^{-1}.

Introduction

In the past several years many tetranuclear manganese complexes have been synthesized and characterized either to mimic the oxygen-evolving center (OEC) of photosystem II (PSII) or to study the ground-state spin frustration that is typical in complexes of this kind.[2] One of the first complexes synthesized contained the $[Mn_4(\mu_3\text{-}O)_2]$ core, with the $[Mn_4O_2(RCOO)_x(bpy)_2]^z$ ($x = 6, 7$; $z = 0, 1+$; R = alkyl or aryl group; bpy = *2,2′*-bipyridine) formulation, where the metals are arranged in either a planar or nonplanar ("butterfly") fashion (Scheme 1) and the metal oxidation states are $Mn^{II}_2Mn^{III}_2$, $Mn^{II}Mn^{III}_3$, or Mn^{III}_4.[3,4]

Scheme 1

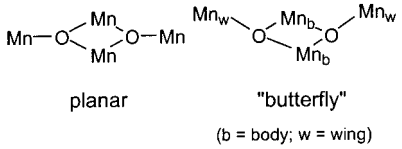

Later, because some reports[5] suggested that the number of nitrogen-based ligands on the Mn atoms of the OEC was either

(1) (a) Departament de Química Inorgànica, Universitat de Barcelona, Spain. (b) Department of Chemistry, Indiana University, Bloomington, Indiana. (c) Department of Chemistry, University of California—San Diego, La Jolla, California.

(2) (a) Que, L., Jr.; True, A. E. In *Progress in Inorganic Chemistry: Bioinorganic Chemistry*; Lippard, S. J., Ed.; J. Wiley & Sons: New York, 1990; Vol. 38, pp 166−181. (b) Pecoraro, V. L. *Photochem. Photobiol.* **1988**, *48*, 249. (c) Christou, G. *Acc. Chem. Res.* **1989**, *22*, 328. (d) Wieghardt, K. *Angew. Chem., Int. Ed. Engl.* **1989**, *28*, 1153. (e) Brudvig, G. W.; Crabtree, R. H. *Prog. Inorg. Chem.* **1989**, *37*, 99.

(3) Christou, G.; Vincent, J. B. *Biochim. Biophys. Acta* **1987**, *895*, 259.

(4) (a) Christmas, C.; Vincent, J. B.; Huffman, J. C.; Christou, G.; Chang, H.-R.; Hendrickson, D. N. *J. Chem. Soc., Chem. Commun.* **1987**, 1303. (b) Vincent, J. B.; Christmas, C.; Huffman, J. C.; Christou, G.; Chang, H.-R.; Hendrickson, D. N. *J. Chem. Soc., Chem. Commun.* **1987**, 236. (c) Vincent, J. B.; Christmas, C.; Chang, H.-R.; Li, Q.; Boyd, P. D. W.; Huffman, J. C.; Hendrickson, D. N.; Christou, G. *J. Am. Chem. Soc.* **1989**, *111*, 2086.

10.1021/ic0010555 CCC: $20.00
Published on Web 02/02/2001

zero, 1N/Mn_4, or 2N/Mn_4, bidentate O- and N-based ligands such as pic^- (anion of the picolinic acid), hqn^- (anion of the 8-hydroxyquinoline), Cl-hqn^- (anion of the 5-chloro-8-hydroxyquinoline), and hmp^- (anion of the 2-(hydroxymethyl)pyridine)[6,7] were used instead of bpy, and the equivalent tetranuclear complexes $[Mn_4O_2(RCOO)_7(L)_2]^+$ were synthesized in which the oxidation state of all the metals was +3. These new compounds had the same structure and magnetic behavior as the bpy derivatives. However, the redox properties were sensitive to the chelate.[6a,7] In contrast, this potential was little affected by variation of the seven carboxylates from acetate to benzoate. This feature was interesting from a bioinorganic point of view, and it was in agreement with the suggestion that the N ligation to the OEC was minimal.[5] As pointed out by Libby et al,[6a] the predominant O ligation to the OEC aggregate may have been "evolutionarily dictated by the need to minimize the oxidation potentials required to access to higher oxidation levels". With this idea in mind, Christou's group prepared three more tetranuclear complexes with only O-based ligation, $[Mn_4O_2(MeCOO)_6(L)_2(dbm)_2]$ (L = py or EtOAc; dbm = anion of the dibenzoylmethane)[8] and $(NBu_4)[Mn_4O_2(PhCOO)_9(H_2O)]$,[9] both with a $[Mn^{III}_4(\mu\text{-}O)_2]$ formulation. The latter is called the "naked butterfly" because in the absence of a chelating ligand such as bpy it possesses instead two carboxylates, one in a monodentate fashion and the other in a rare chelating mode, and a terminal aqua ligand. This is important for the OEC modeling, since this complex presents a water-binding site. Moreover, this feature makes it quite accessible to other reagents and is therefore a good starting point for the synthesis of new, higher nuclearity Mn complexes.[9] At about the same time, a similar complex, which contained only O-donor ligands, $[Mn_4O_2(Ph_3CCOO)_6(OEt_2)_2]$, was prepared by Crabtree and Brudvig,[10] but this presented a mixed-valence $Mn^{II}_2Mn^{III}_2$ formulation. Until now, only one $Mn^{II}Mn^{III}_3$ butterfly complex, $[Mn_4O_2(benzoato)_7(bpy)_2]$, has been reported but without a crystal structure.[4c,11]

The variability of the ground-state spin and the presence of the spin-frustration phenomenon in these tetranuclear manganese complexes have been the objects of considerable study. For Mn_4^{III} complexes, Libby, McCusker, et al. have reported a complete study of their spin frustration.[6a,12] In a paper by Wemple et al. on the $Mn^{II}Mn_3^{III}$ complex,[11] there is also a discussion of spin frustration in this mixed-valence complex.

Scheme 2

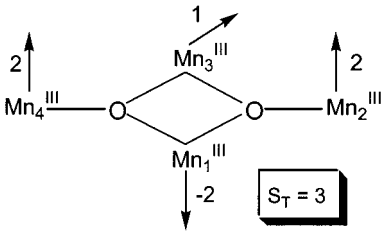

Scheme 3

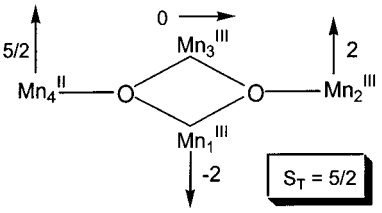

Scheme 3a

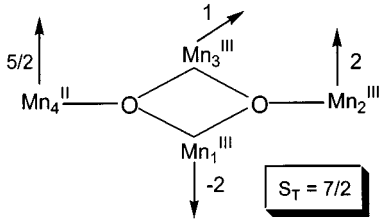

Scheme 3b

Magnetization measurements on these complexes confirm that the ground state is normally $S_T = 3$ because the body−body antiferromagnetic interactions (J_{bb}) are much larger than the body−wingtip interaction (J_{wb}) (for J_{bb} and J_{wb} see Scheme 4). Thus, even though both types of pairwise exchange interaction are antiferromagnetic, the ground state of these complexes has six unpaired electrons. This results from spin frustration. The net result is that the spin alignments of the body ions are frustrated (Scheme 2). In this scheme, Mn1 and Mn3 are of course equivalent by symmetry, and the scheme is thus to be interpreted as showing that the coupling of these Mn ions gives $S_{13} = 1$ rather than $S_{13} = 0$ expected from the antiferromagnetic J_{bb} parameter. The S_{13} resultant spin then couples with the $S_{24} = 4$ to give the resultant $S = 3$ ground state of the complete molecule. A similar interpretation of the other schemes to follow should be made. As Libby et al. pointed out,[6] it is clear that relatively small changes in the J_{wb} and J_{bb} parameters could cause the $S = 2$ or $S = 0$ states to become the ground state.

For the mixed-valence compound $[Mn_4O_2(benzoato)_7(bpy)_2]$ the ground-state spin reported by Wemple et al. is $^5/_2$.[11] This ground state can be rationalized as a perturbation of the $4Mn^{III}$ case mentioned above, caused by addition of one electron to a wingtip Mn atom. There is a significant reduction of the J_{bb} interaction on reduction of a wingtip Mn^{III} to an Mn^{II} ion, the effect transmitted via the oxide ion that bridges the Mn^{III} and Mn^{II} ions, and this appears to be the main factor responsible for the $S = {}^5/_2$ ground state (Scheme 3a). But for this reduced butterfly "had the relative J_{bb} and J_{wb} values remained as they are in the $4Mn^{III}$ complexes, the ground state would have been expected to be $S_T = {}^9/_2 - 1 = {}^7/_2$"[11](Scheme 3b).

Here we report the continuation of the study of this kind of mixed-valent butterfly complex. We describe the syntheses and characterization of two new $Mn^{II}Mn^{III}_3$ complexes, $[Mn_4O_2(2X\text{-}$

(5) (a) Tamura, N.; Ikeuchi, M.; Inoue, Y. *Biochim. Biophys. Acta* **1989**, *973*, 281. (b) Andreasson, L. E. *Biochim. Biophys. Acta* **1989**, *973*, 465.
(6) (a) Libby, E.; McCusker, J. K.; Schmitt, E. A.; Folting, K.; Hendrickson, D. N.; Christou, G. *Inorg. Chem.* **1991**, *30*, 3486. (b) Libby, E.; Folting, K.; Huffman, C. J.; Huffman, J. C.; Christou, G. *Inorg. Chem.* **1993**, *32*, 2549.
(7) Bouwman, E.; Bolcar, M. A.; Libby, E.; Huffman, J. C.; Folting, K.; Christou, G. *Inorg. Chem.* **1992**, *31*, 5185.
(8) (a) Wang, S.; Folting, K.; Streib, W. E.; Schmitt, E. A.; McCusker, J. K.; Hendrickson, D. N.; Christou, G. *Angew. Chem., Int. Ed. Engl.* **1991**, *30*, 305. (b) Wang, S.; Tsai, H.-L.; Folting, K.; Martin, J. D.; Hendrickson, D. N.; Christou, G. *J. Chem. Soc., Chem. Commun.* **1994**, 671.
(9) Wang, S.; Huffman, J. C.; Folting, K.; Streib, W. E.; Lobkovsky, E. B.; Christou, G. *Angew. Chem., Int. Ed. Engl.* **1991**, *30*, 1672.
(10) (a) Kulawiec, R. J.; Crabtree, R. H.; Brudvig, G. W.; Schulte, G. K. *Inorg. Chem.* **1988**, *27*, 1309. (b) Thorp, H. H.; Sarneski, J. E.; Kulawiec, R. J.; Brudvig, G. W.; Crabtree, R. H.; Papaefthymiou, G. C. *Inorg. Chem.* **1991**, *30*, 1153.
(11) Wemple, M. W.; Tsai, H.-L.; Wang, S.; Claude, J. P.; Streib, W. E.; Huffman, J. C.; Hendrickosn, D. N.; Christou, G. *Inorg. Chem.* **1996**, *35*, 6437.
(12) McCusker, J. K.; Schmitt, E. A.; Hendrickon, D. N. High Spin Inorganic Clusters: Spin Frustration in Polynuclear Manganese and Iron Complexes. In *Magnetic Molecular Materials*; Gatteschi, D., Kahn, O., Miller, J. S., Palacio, F., Eds.; NATO ASI Series 198; Kluwer: Dordrecht, 1991; pp 297−319.

PhCOO)$_7$(bpy)$_2$] (X = Cl, Br) **1** and **2**, and the crystal structure of the 2-Cl derivative **1**. This is the first of these reduced butterflies for which the crystal structure has been solved. Susceptibility and magnetization measurements indicate that in both cases the ground-state spin is $^7/_2$ but with low-lying excited states ($^9/_2$, $^5/_2$, $^3/_2$, $^1/_2$) very close in energy, almost degenerate. This demonstrates that a change in ground state can be effected by only a small change in the peripheral ligation. In the absence of structural data on the 2-Br complex, **2**, the analysis, IR bands, and comparison with all 2-Cl and 2-Br derivatives of different nuclearities (trinuclear and dodecanuclear) performed by the authors[13−15] indicate that both complexes are isostructural.

Experimental Section

Materials. All manipulations were performed under aerobic conditions. Reagent grade solvents were used without further purification. Organic reagents were used as received except 2-ClPhCOOH and 2-BrPhCOOH, which were recrystallized from hot water. Yields were calculated from the total available Mn.

Synthesis of [Mn$_4$O$_2$(2-ClPhCOO)$_7$(bpy)$_2$] (1). 2,2′-Bipyridine (0.1 g, 0.6 mmol) in CH_2Cl_2 (5 mL) was added dropwise to a stirred dark-green solution of [Mn$_3$O(2-ClPhCOO)$_6$(py)$_3$][13] (0.54 g, 0.4 mmol) in CH_2Cl_2 (100 mL). A noticeable color change was observed, giving rise to a dark-brown solution. After the solution was stirred for 10 min, a yellow precipitate of an Mn^{II} byproduct was observed. The mixture was left undisturbed in the refrigerator for several minutes until precipitation of the yellow byproduct was judged to be complete. The solid was then removed by filtration. Layering the filtrate with a mixture of ether/hexanes 1:1 (60 mL) and storage at room temperature formed dark-brown, diamond-shaped crystals in up to 80% yield on prolonged storage. The product was collected by filtration, washed with cold ethanol, and dried in air. To avoid any impurity of the yellow byproduct, the dark-brown crystals were recrystallized from CH_2Cl_2/hexanes and, after several days, only the well-shaped crystals were collected, filtered, and dried in air. Several good crystals were left in the mother liquor to make the X-ray crystal structure determination because crystals were found to lose solvent rapidly when dried in air. Anal. Calcd for [Mn$_4$(μ-O)$_2$(μ-2-ClPhCOO)$_7$(bpy)$_2$], $C_{69}H_{44}Cl_7Mn_4N_4O_{16}$ (fw 1653.04 g mol^{-1}): C, 50.13; H, 2.68; N, 3.39; Cl, 15.01; Mn, 13.31. Found: C, 49.9; H, 2.6; N, 3.4; Cl, 15.2; Mn, 13.3. FT-IR data (KBr): 1617(vs), 1602(s), 1561(m), 1473(m), 1436(m), 1391(vs), 1385(vs), 1257(w), 1156(w), 1052(m), 1035(w), 842(w), 800(w), 752(s), 728(w),720(w), 650(m), 637(m), 497(w) cm^{-1}.

Synthesis of [Mn$_4$O$_2$(2-BrPhCOO)$_7$(bpy)$_2$] (2). This new complex was prepared similarly to **1**, starting with 0.4 mmol of 2Br-benzoic acid instead of 2Cl-benzoic acid. All other reagents were the same and used in the same ratio. The yield was 75−80%. Anal. Calcd for [Mn$_4$(μ-O)$_2$(μ-2-BrPhCOO)$_7$(bpy)$_2$], $C_{69}H_{44}Br_7Mn_4N_4O_{16}$ (fw 1964.20 g mol^{-1}): C, 42.19; H, 2.26; N, 2.85; Br, 28.47; Mn, 11.20. Found: C, 42.2; H, 2.2; N, 2.7; Br, 28.2; Mn, 11.2; Cl (possible solvent CH_2Cl_2), 0%. FT-IR data (KBr): 1615(vs), 1595(vs), 1555(m), 1470(m), 1439-(m), 1383(vs), 1156(w), 1052(w), 1028(m), 842(w), 751(s), 728(w), 695(w), 653(m), 635(w), 492(w) cm^{-1}.

Spectral and Magnetic Measurements. IR spectra (4000−400 cm^{-1}) were recorded on KBr pellets with a Nicolet 520 FT-IR spectrometer. Magnetic measurements were carried out in the "Servei de Magnetoquímica (Universitat de Barcelona)" on polycrystalline samples (30−40 mg) with a pendulum type magnetometer−susceptometer (MANICS DSM.8) equipped with an Oxford helium continuous flow cryostat, working in the 4.2−300 K range, and a Drusch EAF 16UE electromagnet. The magnetic field was approximately 1.2 T. The diamagnetic corrections were evaluated from Pascal's constants. To guarantee the accuracy of results, especially in the low-temperature range, magnetic susceptibility and magnetization measurements were also made with a Quantum Design MPMS superconducting quantum interference device (SQUID) susceptometer operating at a magnetic field of 0.5 T between 2 and 300 K. The fit of the magnetic susceptibility was carried out by using the MINUIT minimization program of the CERN program libray (v. 92.1), CERN, Geneva, which ensures the accuracy of results through the command IMPROVE so that the minimum can be calculated. Magnetization measurements (to calculate the ground-state and its anisotropy) were carried out with the same Quantum Design MPMS SQUID susceptometer operating at 2.0−30 K between 0.2 and 5 T. EPR spectra were recorded on powder samples at X-band frequency with a Bruker 300E automatic spectrometer, varying the temperature between 4 and 77 K.

Table 1. Crystallographic Data for [Mn$_4$O$_2$(2·ClPhCOO)$_7$(bpy)$_2$]·3CH$_2$Cl$_2$ (**1**)

empirical formula	$C_{69}H_{44}Cl_7Mn_4N_4O_{16}\cdot 3CH_2Cl_2$
fw	1907.84
space group	$P2_1/n$
temp (°C)	−170
a (Å)	19.849(8)
b (Å)	13.908(5)
c (Å)	30.722(10)
β (deg)	107.35(2)
V (Å^3)	8094.61
Z	4
λ (Å)	0.710 69
ρ_{calcd} (g cm^{-3})	1.566
μ (mm^{-1})	1.1037
$R(F)^a$	0.0941
$R_w(F)^b$	0.0937

^{a} $R = \sum||F_0| - |F_c||/\sum|F_0|$. ^{b} $R_w = [\sum w(|F_0|^2 - |F_c|^2)/\sum w|F_0|^2]^{1/2}$.

X-ray Crystallography and Structure Solution. A suitable crystal was selected and attached to a glass fiber using silicone grease. It was then transferred to the goniostat of a locally modified Picker four-circle diffractometer at approximately −170 °C. Details of the diffractometry, low-temperature facilities, and computational procedures used by the Molecular Structure Center (Indiana University, Bloomington) are available elsewhere.[16] A preliminary search for peaks and then analysis using the programs DIRAX and TRACER revealed a primitive monoclinic unit cell. Following the data collection the conditions $h + l = 2n$ for $h0l$ and $k = 2n$ for $0k0$ uniquely determined the space group as $P2_1/n$ (No. 14). Data collection parameteres are summarized in Table 1. After correction for absorption, data processing gave a unique set of 10 624 reflections and a residual of 0.060 for the averaging of 9271 reflections observed more than once. Four standard reflections (6 0 0, 0 −8 0, 0 0 10, −4 −5 12) measured every 300 reflections showed no significant trends. Because of the long c axis, a rather narrow scan had to be used; some reflections showing evidence of overlap were rejected early in the data processing. Unit cell dimensions were determined by a least-squares fit of the setting angles for 54 carefully centered reflections having 2θ values between 23° and 30°.

The structure was solved using a combination of direct methods (MULTAN-78) and Fourier techniques. The four Mn atoms and several of the Cl atoms were located in the initial E map. The remaining non-hydrogen atoms were located in subsequent iterations of least-squares refinement followed by difference Fourier map calculations. Disorder was observed in the chlorine positions on two of the ortho chlorobenzoate ligands (Cl(36) 65%, Cl(37) 35%, Cl(77) 65%, and Cl(78) 35%). In addition to the molecule of interest the asymmetric unit was found to contain two well-ordered molecules of CH_2Cl_2 as well as very severely disordered solvent molecules assumed to be CH_2Cl_2, which had been used as a solvent. Hydrogen atoms were introduced in fixed calculated positions with the number of isotropic thermal parameters equal to 1 plus the isotropic equivalent of the parent atom.

During the least-squares refinement a carbon atom in one of the benzene rings failed to converge properly when anisotropic thermal

(13) Ribas, J.; Albela, B.; Stoeckli-Evans, H.; Christou, G. *Inorg. Chem.* **1997**, *36*, 2352.
(14) Albela, B. Ph.D. Thesis, University of Barcelona, Barcelona, Spain, 1996.
(15) Aubin, S. M. J.; Ruiz, D.; Rumberger, E.; Sun, Z.; Albela, B.; Wemple, M. W.; Dilley, N. R.; Ribas, J.; Maple, M. B.; Christou, G.; Hendrickson, D. N. *Mol. Cryst. Liq. Cryst.* **1999**, *335*, 1083.
(16) Chisholm, M. H.; Folting, K.; Huffman, J. C.; Kirkpatrick, C. C. *Inorg. Chem.* **1984**, *23*, 1021.

parameters were used. For the remainder of the refinement C(21) was kept isotropic. The least-squares refinement was completed using anisotropic thermal parameters on all but C(21) in the main molecule, as well as on the ordered solvent molecules. The disordered solvent was refined using isotropic thermal parameters. The final $R(F)$ was 0.0941 for 1009 total variables.

The final difference map contained a peak of 2 e/Å^3 at 0.8 Å from C(21). Attempts at fitting this peak to a chemically sensible disorder model failed. The next-highest peaks of about 1 e/Å^3 were located in the area of the disordered solvent.

Results and Discussion

Syntheses. The preparation of $[Mn_4O_2(2\text{-X-benzoato})_7(bpy)_2]$ resulted from an investigation of the reaction between $[Mn_3O(2\text{-X-benzoato})_6(py)_3]$[13] and 2,2-bipyridine. This reaction was studied by Vincent et al.[4c] using two analogous compounds $[Mn_3O(R{-}COO)_6(py)_2(H_2O)]$ (R = Ph, 3-MePh). Wemple et al. reported a magnetic study of the benzoato complex.[11] According to Vincent,[4c] treatment of $[Mn_3O(benzoato)_6(py)_2(H_2O)]$ with approximately 3 equiv of bpy yielded the new $[Mn_4O_2(benzoato)_7(bpy)_2]$:

$$^4/_3[Mn_3O(benzoato)_6(py)_2(H_2O)] + 2bpy \rightarrow [Mn_4O_2(benzoato)_7(bpy)_2] + PhCOOH + {}^2/_3H_2O + {}^8/_3py \quad (1)$$

The average metal oxidation state of the product (+2.75) is greater than the Mn_3O reagent (+2.67), suggesting either involvement of atmospheric O_2 or, more likely, a lower oxidation-state (Mn^{II}) byproduct. The corresponding 3-Me-benzoate derivative can be prepared in an analogous manner. No crystal structure has been reported for either of these two complexes. In a previous study on polynuclear mixed-valence manganese complexes with 2-X benzoato derivatives (X = F, Cl, Br)[14] two main tendencies were observed with these ligands: (a) the 2-Cl-benzoic acid shows a marked tendency to give good crystals and (b) in all series, the 2-Cl and 2-Br-benzoic derivatives are isostructural, although the 2-Br derivatives are less crystalline. For this reason, the reaction of the Mn_3O trinuclear complexes with bpy has been studied for the 2-Cl and 2-Br derivatives. In both cases the reaction takes place in an identical manner, giving the tetranuclear Mn_4O_2 product and a yellow byproduct. The latter is very insoluble in CH_2Cl_2 and all common solvents (including water) and, although it is impure, is a trinuclear Mn^{II} complex of formula $[Mn^{II}_3(2\text{-X-benzoato})_6(bpy)_2]$. This kind of trinuclear complex has been described in the literature; the acetato derivative was reported by Menage et al.[17] and the benzoato by Shake et al.[18] The $[Mn^{II}_3(2\text{-Cl-benzoato})_3(bpy)_2]$ complex has been prepared by direct synthesis, giving IR spectra very similar to that obtained starting from the trinuclear Mn_3O complex.[14] Thus, although not balanced owing to possible unknown byproducts, the reaction that takes place in the synthesis can be summarized as

$$[Mn_3O(2\text{-X-benzoato})_6(py)_3] + bpy \rightarrow [Mn_4O_2(2\text{-X-benzoato})_7(bpy)_2] + [Mn^{II}_3(2\text{-X-benzoato})_3(bpy)_2] \quad (2)$$

Description of the Structure of $[Mn_4(\mu\text{-O})_2(\mu\text{-2-ClPhCOO})_7(bpy)_2]\cdot 3CH_2Cl_2$ (1). $[Mn_4(\mu\text{-O})_2(\mu\text{-2-ClPhCOO})_7(bpy)_2]\cdot 3CH_2Cl_2$, **1**, is the first report of a mixed-valence $Mn^{III}_3Mn^{II}$ complex characterized by X-ray diffraction. The structure of **1**, displayed in Figure 1, is similar to that of complexes with the core $[Mn^{III}_4(\mu_3\text{-O})_2]^{8+}$ reported in the literature.[4b−d,6a,7,9] The structure consists of four manganese atoms linked by two μ_3-oxo bridges. The peripheral ligands are seven carboxylates and two amines, giving rise to a distorted octahedral environment in all Mn atoms. Each terminal Mn is bridged to a central Mn by either one or two μ_2-carboxylate groups. Six of the carboxylates are of this kind, whereas the seventh links the two central manganese atoms. An alternative view of the carboxylate arrangement is as follows: four of them are approximately in the plane of the central $[Mn_2(\mu_3\text{-O})_2]$ rhombus, while the remaining carboxylates are perpendicular to this "plane". Two of the latter are carboxylates that bridge a terminal and a central Mn, and the other one, which is opposite the former two, corresponds to the carboxylate group that bridges the two central Mn atoms. The two bipyridine molecules are also perpendicular to the plane of the central rhombus (Figure 1). The core of the complex is depicted in Figure 2. Relevant bond distances and angles are collected in Table 2. The structure of this core is known as a "butterfly" arrangement; Mn(1) and Mn(2) occupy the "body" or "backbone" positions, and Mn(3) and Mn(4) occupy the "wing-tip" sites. O(5) and O(6) triply bridge each Mn_3 "wing". The core can also be considered as two edge-sharing Mn_3O units in a nonplanar arrangement. Each of these Mn_3O entities can be compared with the precursor trinuclear $[Mn^{II}Mn^{III}_2(\mu_3\text{-O})]$ complexes reported elsewhere.[13] However,

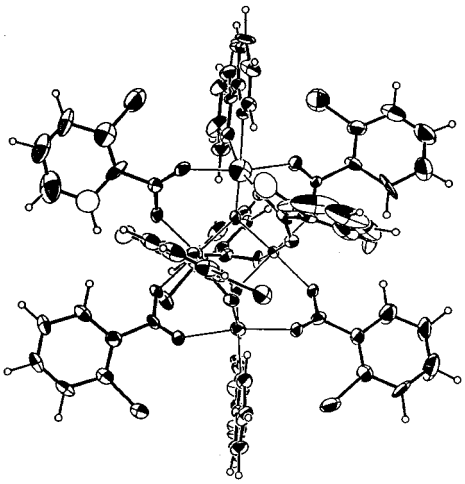

Figure 1. ORTEP drawing of $[Mn_4O_2(2\text{-Cl-benzoato})_7(bpy)_2]$ (**1**). The atom labeling scheme is given in Figure 2.

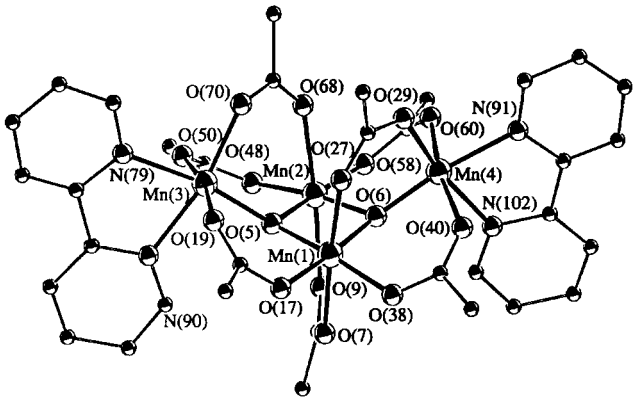

Figure 2. Drawing of the core of $[Mn_4O_2(2\text{-Cl-benzoato})_7(bpy)_2]$ (**1**) with the atom labeling scheme. All benzoate rings have been omitted for clarity.

(17) Menage, S.; Vitols, S. E.; Bergerat, P.; Codjovi, E.; Kahn, O.; Girerd, J. J.; Guillot, M.; Solans, X.; Calvet, T. *Inorg. Chem.* **1991**, *30*, 2666.
(18) Shake, A. R. Ph.D. Thesis, University of Indiana, Bloomington, IN, 1990; Chapter 5.

Table 2. Selected Bond Distances (Å) and Angles (deg) for $[Mn_4O_2(2\text{-}ClPhCOO)_7(bpy)_2]\cdot 3CH_2Cl_2$ (**1**) with Estimated Standard Deviations in Parentheses

Mn(1)−O(5)	1.858(5)	Mn(3)−O(5)	1.945(14)
Mn(1)−O(6)	1.896(7)	Mn(3)−O(19)	2.120(5)
Mn(1)−O(7)	2.186(14)	Mn(3)−O(50)	2.137(4)
Mn(1)−O(17)	1.982(8)	Mn(3)−O(70)	2.013(10)
Mn(1)−O(27)	2.223(13)	Mn(3)−N(79)	2.153(16)
Mn(1)−O(38)	1.969(7)	Mn(3)−N(90)	2.146(10)
Mn(2)−O(5)	1.864(8)	Mn(4)−O(6)	1.847(5)
Mn(2)−O(6)	1.905(4)	Mn(4)−O(29)	1.965(15)
Mn(2)−O(9)	2.263(14)	Mn(4)−O(40)	2.171(5)
Mn(2)−O(48)	1.9933(21)	Mn(4)−O(60)	2.147(5)
Mn(2)−O(58)	1.976(8)	Mn(4)−N(91)	2.089(6)
Mn(2)−O(68)	2.171(15)	Mn(4)−N(102)	2.080(18)
Mn(1)−Mn(2)	2.792(2)	Mn(1)−Mn(4)	3.290(3)
Mn(1)−Mn(3)	3.414(3)	Mn(2)−Mn(4)	3.368(2)
Mn(2)−Mn(3)	3.339(4)	Mn(3)−Mn(4)	5.572(4)
O(5)−Mn(1)−O(6)	83.8(3)	O(5)−Mn(3)−O(19)	92.2(4)
O(5)−Mn(1)−O(7)	87.9(4)	O(5)−Mn(3)−O(50)	91.6(4)
O(5)−Mn(1)−O(17)	94.3(3)	O(5)−Mn(3)−O(70)	97.8(4)
O(5)−Mn(1)−O(27)	97.6(4)	O(5)−Mn(3)−N(79)	169.6(4)
O(5)−Mn(1)−O(38)	173.7(5)	O(5)−Mn(3)−N(90)	94.1(6)
O(6)−Mn(1)−O(7)	91.3(4)	O(19)−Mn(3)−O(50)	169.72(23)
O(6)−Mn(1)−O(17)	175.4(6)	O(19)−Mn(3)−O(70)	100.7(3)
O(6)−Mn(1)−O(27)	90.7(4)	O(19)−Mn(3)−N(79)	87.2(4)
O(6)−Mn(1)−O(38)	96.2(3)	O(19)−Mn(3)−N(90)	86.08(27)
O(7)−Mn(1)−O(17)	92.9(4)	O(50)−Mn(3)−O(70)	88.3(3)
O(7)−Mn(1)−O(27)	174.31(23)	O(50)−Mn(3)−N(79)	87.4(4)
O(7)−Mn(1)−O(38)	85.8(4)	O(50)−Mn(3)−N(90)	84.12(25)
O(17)−Mn(1)−O(27)	85.4(4)	O(70)−Mn(3)−N(79)	92.5(5)
O(17)−Mn(1)−O(38)	86.2(3)	O(70)−Mn(3)−N(90)	166.1(5)
O(27)−Mn(1)−O(38)	88.7(4)	N(79)−Mn(3)−N(90)	75.5(6)
O(5)−Mn(2)−O(6)	83.41(28)	O(6)−Mn(4)−O(29)	99.4(5)
O(5)−Mn(2)−O(9)	89.0(4)	O(6)−Mn(4)−O(40)	93.86(22)
O(5)−Mn(2)−O(48)	97.18(26)	O(6)−Mn(4)−O(60)	92.43(19)
O(5)−Mn(2)−O(58)	176.75(7)	O(6)−Mn(4)−N(91)	170.1(7)
O(5)−Mn(2)−O(68)	91.4(5)	O(6)−Mn(4)−N(102)	91.7(5)
O(6)−Mn(2)−O(9)	85.4(4)	O(29)−Mn(4)−O(40)	88.2(4)
O(6)−Mn(2)−O(48)	172.0(6)	O(29)−Mn(4)−O(60)	98.2(4)
O(6)−Mn(2)−O(58)	93.44(28)	O(29)−Mn(4)−N(91)	90.6(5)
O(6)−Mn(2)−O(68)	99.4(4)	O(29)−Mn(4)−N(102)	166.60(10)
O(9)−Mn(2)−O(48)	86.7(4)	O(40)−Mn(4)−O(60)	170.2(4)
O(9)−Mn(2)−O(58)	91.5(4)	O(40)−Mn(4)−N(91)	86.59(22)
O(9)−Mn(2)−O(68)	175.18(10)	O(40)−Mn(4)−N(102)	83.5(4)
O(48)−Mn(2)−O(58)	86.04(25)	O(60)−Mn(4)−N(91)	85.93(19)
O(48)−Mn(2)−O(68)	88.5(4)	O(60)−Mn(4)−N(102)	88.8(4)
O(58)−Mn(2)−O(68)	88.3(5)	N(91)−Mn(4)−N(102)	78.5(5)
Mn(1)−O(5)−Mn(2)	97.2(4)	Mn(1)−O(6)−Mn(2)	94.6(3)
Mn(1)−O(5)−Mn(3)	127.7(5)	Mn(1)−O(6)−Mn(4)	123.0(3)
Mn(2)−O(5)−Mn(3)	122.4(5)	Mn(2)−O(6)−Mn(4)	127.7(5)

the Mn_3O units are not perfectly planar in the "butterfly" complex; the oxygen atom is displaced slightly below the plane of the Mn_3 triangle. Moreover, these Mn_3O units are more asymmetric, as shown at the bond angles at the triply bridging oxygen atoms. The Mn(1)−O(5)−Mn(2) (97.2°) and Mn(1)−O(6)−Mn(2) (94.6°) angles are significantly smaller than the other Mn−O−Mn angles, which are in the range 122.4−127.7°.

Complex **1** presents a mixed-valence oxidation state $[Mn^{II}\text{-}Mn^{III}_3(\mu_3\text{-}O)_2]^{7+}$. Mn(3) was assigned as the Mn^{II} atom, on the basis of its longer Mn−ligand distances compared with the other Mn (see Table 2). For example, the distance to the μ_3-oxo is significantly greater for this manganese ($d_{Mn(3)-O(5)} = 1.946$ Å) than for the other terminal manganese assigned as Mn^{III} ($d_{Mn(4)-O(6)} = 1.848$ Å).

The assignment of the Mn oxidation states was confirmed by the presence of a Jahn−Teller (JT) axial elongation at the Mn(1), Mn(2), and Mn(4) atoms, as expected for an octahedral Mn^{III} (high-spin d^4). The JT axes at Mn(1) (O(27)−Mn(1)−O(7)) and Mn(2) (O(68)−Mn(2)−O(9)) are nearly perpendicular to the central $[Mn_2(\mu_3\text{-}O)_2]$ rhombus, whereas the JT axis at Mn(4) (O(60)−Mn(4)−O(40)) is nearly coplanar with it.

Scheme 4

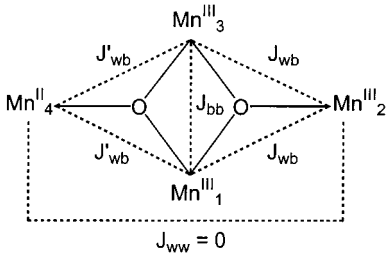

However, Mn(3) shows distances similar to those of all the ligands, as expected for an Mn^{II} ion.

The "butterfly" arrangement leads to diverse Mn···Mn distances, which depend on the number of μ-oxo and μ-carboxylate bridges between the two metal centers and on the oxidation state of each Mn atom. The central Mn(1)···Mn(2) separation is the shortest (2.792 Å), whereas the Mn···Mn distances between a terminal and a central Mn are in the range 3.29−3.42 Å. This is in agreement with the number of μ-oxo bridges: two in the former and one in the latter. Christou and Vincent[19] have summarized that in oxo-bridged systems Mn···Mn separations are about 2.7−2.8 Å if bridged by two oxo groups and about 3.3 Å if bridged by only one, which is consistent with our results. The distances between a central and a terminal Mn are slightly larger for $Mn^{II}_t\cdots Mn^{III}_c$ (3.341, 3.416 Å) than for $Mn^{III}_t\cdots Mn^{III}_c$ (3.291, 3.368 Å), which is consistent with the oxidation state of the metal centers. Moreover, for each Mn···Mn pair two different distances are observed. The shorter Mn···Mn separation corresponds to the pair bridged by two carboxylate groups (Mn(1)−Mn(4), Mn(2)−Mn(3)), whereas the larger distance corresponds to those linked by only one carboxylate bridge (Mn(1)−Mn(3), Mn(2)−Mn(4)).

Magnetochemical Studies

The study of the magnetic properties of $[Mn_4(\mu_3\text{-}O)_2(\mu\text{-}2\text{-}ClPhCOO)_7(bpy)_2]$ was performed taking into account the discussion by Wemple et al.[11] for the benzoato analogue for which, in the absence of a crystal structure, it was assumed that the Mn^{II} was located in a wingtip position. The structure of **1** has demonstrated that this assumption is perfectly correct. The $[Mn_4O_2]^{7+}$ core of **1** thus has idealized C_s symmetry, requiring three J parameters to describe the magnetic exchange interactions betweeen the four metal centers (Scheme 4). A fourth exchange parameter J_{ww} describing the interaction between the two wingtip Mn atoms is taken as zero, as is customary for such butterfly complexes, given the large distance betweeen these metal atoms.[4c]

J_{bb} corresponds to the exchange between the two central Mn atoms bridged by two μ-oxo, whereas J_{wb} and J_{wb}' account for the interactions between $Mn^{III}\cdots Mn^{III}$ and $Mn^{II}\cdots Mn^{III}$ pairs that are bridged by only one μ-oxo. The presence of either one or two carboxylate bridges between the Mn was not considered to have a significant effect on the magnetic coupling between these two centers. As indicated above, the J_{ww} parameter was assumed to be negligible. The Heisenberg spin Hamiltonian corresponding to this exchange scheme is given by

$$H = -2J_{bb}S_1S_3 - 2J_{wb}(S_1S_2 + S_2S_3) - 2J_{wb}'(S_1S_4 + S_3S_4) \quad (3)$$

(19) Christou, G.; Vincent, J. B. In *ACS Symposium Series 372*; Que, L., Ed.; American Chemical Society: Washington, DC, 1988; Chapter 12, pp 238−255.

Table 3. Distribution of Spin States for $[Mn^{III}_3Mn^{II}O_2]$ Complexes

S_T	n [a]	$n(2S_T + 1)$ [b]
$^{17}/_2$	1	18
$^{15}/_2$	3	48
$^{13}/_2$	6	84
$^{11}/_2$	10	120
$^{9}/_2$	15	150
$^{7}/_2$	18	144
$^{5}/_2$	18	108
$^{3}/_2$	15	60
$^{1}/_2$	9	18

[a] 95 individual spin states. [b] $\sum[n(2S_T + 1)] = 750$, overall degeneracy of the spin system.

Unfortunately, a Kambe vector coupling scheme[20] is not possible for this system. Therefore, a full-matrix diagonalization approach would be required to obtain the eigenvalues of this spin Hamiltonian. To avoid the full-diagonalization approach to find the interaction parameters, the spin Hamiltonian of this system (eq 3) can be simplified by introducing an approximation, namely, that all exchange interactions between terminal and central Mn atoms are equivalent, i.e., $J_{wb} = J_{wb}'$.[11] This is reasonable because exchange interactions between $[Mn^{III}(\mu_3\text{-}O)Mn^{III}]$ and $[Mn^{III}(\mu_3\text{-}O)Mn^{II}]$ units are known to be comparable, -2.7 to -10.2 cm^{-1} and -1.5 to -6.5 cm^{-1}, respectively.[11] With this approximation, the spin Hamiltonian of eq 3 simplifies to

$$H = -2J_{wb}(S_1S_2 + S_2S_3 + S_3S_4 + S_4S_1) - 2J_{bb}S_1S_3 \quad (4)$$

which is the same as that employed to analyze the magnetic interactions within $[Mn_4(\mu_3\text{-}O)_2]^{6+,8+}$ cores of the other tetranuclear complexes with $2Mn^{II}-2Mn^{III}$ or $4Mn^{III}$ oxidation states and idealized C_{2v} symmetry.

In this Hamiltonian it is assumed that $J_{12} = J_{23} = J_{34} = J_{41} = J_{wb}$, $S_1 = S_2 = S_3 = 2$, and $S_4 = {}^5/_2$. In addition, the effects of zero-field splitting have not been considered. With these simplifications the eigenvalues of the spin Hamiltonian may be determined by using the Kambe vector coupling method[20] with the following coupling scheme:

$$S_{13} = S_1 + S_3; \quad S_{24} = S_2 + S_4; \quad S_T = S_{13} + S_{24}$$

The spin Hamiltonian of eq 4 can now be expressed in the equivalent form of

$$H = -J_{wb}(S_T^2 - S_{13}^2 - S_{24}^2) - J_{bb}(S_{13}^2 - S_1^2 - S_3^2) \quad (5)$$

The energies of the spin states, which are eigenvalues of the Hamiltonian in this coupling scheme, are given by

$$E = -J_{wb}[S_T(S_T + 1) - S_{13}(S_{13} + 1) - S_{24}(S_{24} + 1)] - J_{bb}[S_{13}(S_{13} + 1)] \quad (6)$$

The overall degeneracy of this spin system is 750, made up of 95 individual spin states ranging from $S_T = {}^1/_2$ to $S_T = {}^{17}/_2$ (Table 3).

A theoretical expression for the molar paramagnetic susceptibility (χ_M) vs temperature was derived for complex **1** by using the van Vleck equation[21] and assuming an isotropic g value. This expression was used to fit the experimental χ_M vs T data for **1** and **2**, and the parameters varied were J_{wb}, J_{bb}, and g. On the other hand, a complete full-diagonalization treatment was also used in which the parameters varied were $J_{wb}(Mn^{III}-Mn^{III})$, $J_{wb}'(Mn^{II}-Mn^{III})$, J_{bb}, and g. In both cases, only data for temperatures above 40 K were considered in the fit to avoid complications at low temperature from zero-field splitting of $S_T \geq {}^3/_2$ terms.[22] In fact, another fit employing the χ_M data at $\geq$20 K was also made, but the final R factor was worse. The fit parameters are indicated in Table 4 for 2-Cl and 2-Br complexes. The fit is shown as a solid line in Figure 3. By use of these values, the ground state was determined by the two methods (Kambe and full-diagonalization approaches). By use of the format (S_T, S_{13}, S_{24}) in the Kambe approach, the ground state is a $^7/_2$ state arising from ($^7/_2$, 1, $^9/_2$). With the full-diagonalization method the ground state is also $^7/_2$ for **1** and **2**. In this case, the energy diagram is given in Figure 4.

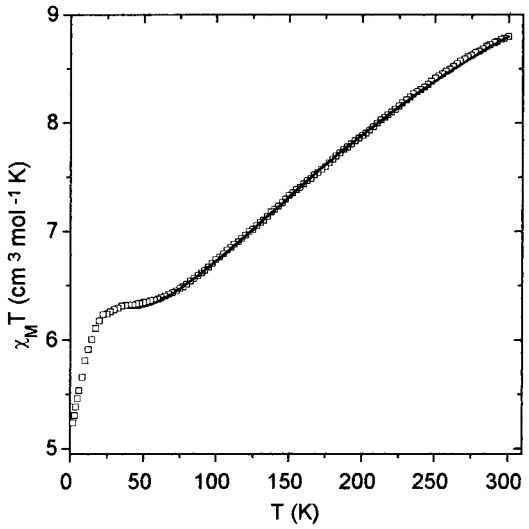

Figure 3. $\chi_M T$ vs T curve for $[Mn_4O_2(2\text{-Cl-benzoato})_7(bpy)_2]$ (**1**). Solid line represents the best fit with the full-diagonalization matrix method. The curve for **2** is analogous. See text (Table 4) for the best-fitted J and g values.

The J_{bb} and J_{wb} values obtained for **1** and **2** are within the range expected for Mn(II/III) complexes bridged by μ_3-O^{2-} ions (Table 4). The J_{bb} value (about -23 cm^{-1}) is within the range (-2.8 to -24.6 cm^{-1}) observed for other $[Mn^{III}(\mu_3\text{-}O)Mn^{III}]$ units.[11] The J_{wb} values are almost equivalent in the full-diagonalization method in which these two values are unconstrained. These values (about -5 cm^{-1}) are within the range for both these types of interaction, -1.5 to -6.5 cm^{-1} for Mn^{II}/Mn^{III} and -2.7 to -10.2 cm^{-1} for Mn^{III}/Mn^{III}.[11] Thus, the hypothesis proposed by Wemple et al. for the analysis of the benzoato derivative[11] for which the two J_{wb} values were assumed to be equal agrees with the results of the full-diagonalization method in which both J_{wb} values are found to be essentially identical. The most marked difference among **1**, **2**, and the benzoato analogue[11] lies in the magnitude of the J values. We will comment on this comparison in the next section.

Variability of the Ground State. Spin Frustration in $[Mn_4O_2]^{7+}$ Complexes. In the Kambe approach, which is shown to be valid in this kind of tetranuclear manganese complex (at least for **1**, **2**, and the benzoato analogue), the energies of the ground state (in units of J_{bb}) vs the J_{wb}/J_{bb} ratio can be rationalized (Figure 5). According to this ratio, the ground-state spin could be $^9/_2$ for a very small J_{wb}/J_{bb} ratio (0$-$0.2). When J_{wb}/J_{bb} lies approximately between 0.2 and 0.35, the ground-

(20) Kambe, K. *J. Phys. Soc. Jpn.* **1950**, *5*, 48.
(21) Van Vleck, J. H. *The Theory of Electric and Magnetic Susceptibilities*; Oxford University Press: London, 1932.
(22) The series of calculations were made using the computer program CLUMAG, which uses the irreductible tensor operator formalism (ITO)): Gatteschi, D.; Pardi, L. *Gazz. Chim. Ital.* **1993**, *123*, 231.

Table 4. Best-Fit Parameters (J in cm^{-1}) for $[Mn_4O_2(2\text{-ClPhCOO})_7(bpy)_2]$ (**1**) and $[Mn_4O_2(2\text{-BrPhCOO})_7(bpy)_2]$ (**2**), Employing the Kambe Method or a Full-Diagonalization Matrix Method (See Text for Details)

complex	J_{bb}	$J_{wb}(Mn^{III}-Mn^{III})$	$J_{wb}'(Mn^{II}-Mn^{III})$	g	R
1, full diagonalization	−23.2	−4.97	−4.84	1.93	1.9×10^{-6}
1, Kambe method	−23.8	−4.31	−4.31	1.90	3.4×10^{-6}
2, full diagonalization	−22.8	−4.85	−4.74	1.92	2.0×10^{-6}
2, Kambe method	−22.5	−4.51	−4.51	1.91	2.9×10^{-6}

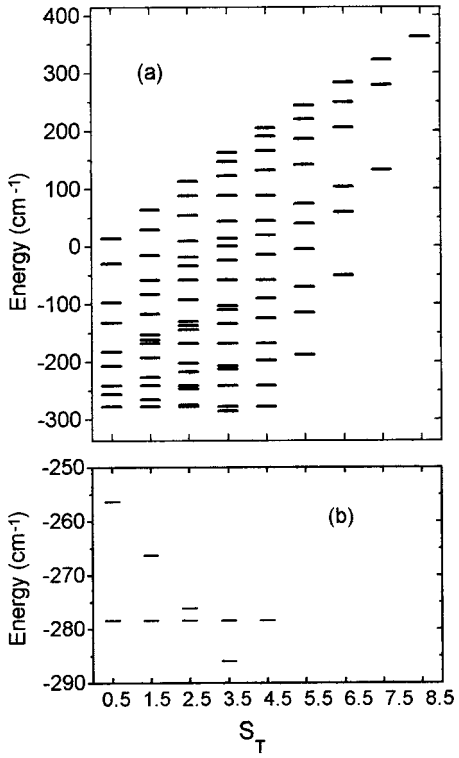

Figure 4. (a) Diagram of all energy values for all S_T spin values. The ground-state spin corresponds to $S_T = {}^7/_2$ (energy = −286 cm^{-1} by full-diagonalization matrix method). The complete degeneracy is given in Table 4. (b) Energy diagram of only the ground state and the low-lying excited states, showing the degeneracy of the $S_T = {}^1/_2$, ${}^3/_2$, ${}^5/_2$, ${}^7/_2$, and ${}^9/_2$ at 279 cm^{-1}.

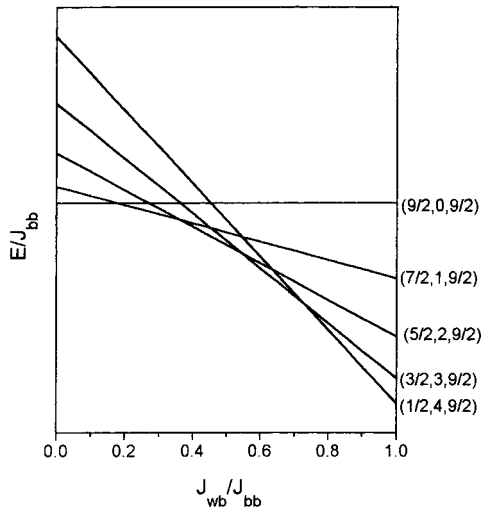

Figure 5. Variation in energy of the low-lying spin states of $[Mn_4O_2(2\text{-Cl-benzoato})_7(bpy)_2]$ (**1**) as a function of J_{wb}/J_{bb}, showing the change in ground state (between parentheses are S_T, S_{13}, S_{24}).

state spin is ${}^7/_2$. When J_{wb}/J_{bb} lies between 0.35 and 0.5, the ground-state spin is ${}^5/_2$, and for higher J_{wb}/J_{bb} values the ground-state spin could be ${}^3/_2$ or even ${}^1/_2$ (J_{wb}/J_{bb} between 0.75 and 1). The benzoato complex reported by Wemple et al.[11] has a

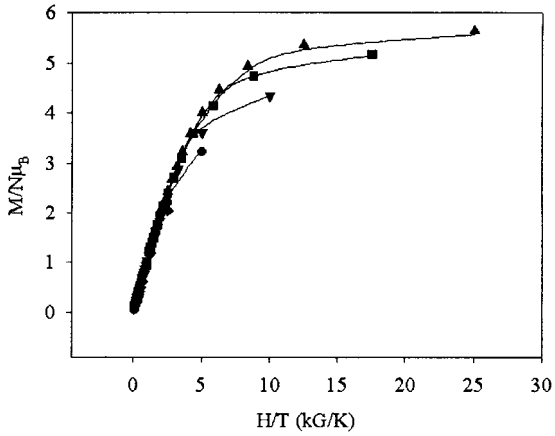

Figure 6. Plot of the reduced magnetization $M/(N\beta)$ vs H/T for $[Mn_4O_2(2\text{-Cl-benzoato})_7(bpy)_2]$ (**1**). Fields are 1, 2, 3.5, and 5 T).

$J_{wb}/J_{bb} \approx 0.4$, which corresponds to a ground-state spin $S_T = {}^5/_2$, in agreement with magnetization data. In the two new complexes reported here, **1** and **2**, $J_{wb}/J_{bb} \approx 0.2$, which should correspond to a ground-state spin of ${}^7/_2$, which agrees with the ground-state spin derived from the fit (Kambe's method and full-diagonalization approach). In the absence of structural data for the benzoato complex, magnetostructural correlations between the benzoato and the 2-halobenzoato complexes are impossible to do. For 2-Cl (**1**) and 2-Br (**2**) complexes, J and J_{wb}/J_{bb} values are the same, and thus, the equivalence and isostructural character of these two complexes can be deduced.

Magnetization vs Field Studies. The ground state can be determined by examining the magnetization of the compound at low temperatures as a function of the applied magnetic field. Plots of $M/(N\beta)$ versus H/T carried out at various magnetic fields for complex **1** are shown in Figure 6. If only one state is populated at these temperatures and applied fields, the non-superimposability of the six isofield data sets indicates the presence of zero-field splitting (ZFS) in the ground state. From Figure 6 it is clear that the $M/(N\beta)$ value tends to 6 (the highest experimental value is 5.64 at the highest field, 5 T). This reduced magnetization is close to saturation under these conditions. The value of 5.6 is consistent with an $S_T = {}^7/_2$ ground state and a g value less than 2, as expected for Mn. This value is not consistent with an $S_T = {}^5/_2$ ground state. The benzoato analogue,[11] whose reduced magnetization is almost saturated at a value of 4.3, has an $S_T = {}^5/_2$ ground state, as found in the susceptibility measurements and in the J_{wb}/J_{bb} ratio.

Emphasis should be given to the reasoning postulated by Wemple et al. in the benzoato complex.[11] In an attempt to rationalize the $S_T = {}^5/_2$ ground state as a perturbation of the $4Mn^{III}$ case caused by addition of one electron to a wingtip Mn atom, they indicate that if the relative J_{bb} and J_{wb} values remained as they are in the $4Mn^{III}$ complexes, the ground state would have been expected to be $S_T = {}^7/_2$. The J values obtained for $[Mn^{III}{}_4O_2(acetato)_7(bpy)_2](ClO_4)$ are $J_{bb} = -23.5$ cm^{-1} and $J_{wb} = -7.8$ cm^{-1}.[4c] These values are very similar to those found for the 2-Cl, **1**, and 2-Br, **2**, complexes. Thus, the ground-state S_T of ${}^7/_2$ for **1** and **2** confirms all asumptions made by Wemple

et al.[11] and allows us to conclude that the variability of the ground-state spin of these complexes is due to spin frustration. Further, the experimental magnetization data can be fitted by calculating the theoretical expression for a given ground state. The energies of the spin sublevels (M_S) are obtained by diagonalization of the spin Hamiltonian matrix, including Zeeman interactions and axial zero-field splitting (D), and use of a full powder average. Solid lines in Figure 6 show the best fit, obtained for an $S = {}^7/_2$ ground state. The fitting parameters were found to be $g = 1.73$, $D = -0.60$ cm^{-1}. Care must be exercised in these calculations in this kind of tetranuclear complex because it is assumed that only one state is thermally populated with a total spin S. In our calculations with the full-diagonalization matrix method, when the data are fit only for $\geq$40 K the ground state $S = {}^7/_2$ seems to be slightly separated from $S_T = {}^5/_2$, ${}^3/_2$, and ${}^1/_2$, which are degenerate (Figure 4). But, for example, when the fit was made with the data for $\geq$25 K, even if the R factor value is slightly worse, the $S_T = {}^7/_2$ is almost degenerate with $S_T = {}^9/_2$, ${}^5/_2$, ${}^3/_2$, and ${}^1/_2$ (there is a difference of only 3−4 cm^{-1}). Thus, even if the J values do not vary appreciably for $\geq$40 K or $\geq$25 K, the degeneracy of all these states is more marked when the susceptibility values are cut at lower temperature. Taking into account that it is not possible to know exactly when the susceptibillity values must be cut, it is clear, nevertheless, that the difference in energy between $S_T = {}^7/_2$ and $S_T = {}^5/_2$ or lower is very small. Thus, at all the temperatures in which the magnetization is made, the assumption of only one populated state should be treated with caution.

EPR Spectra. $[Mn_4O_2(2\text{-ClPhCOO})_7(bpy)_2]$, **1**, and $[Mn_4O_2(2\text{-BrPhCOO})_7(bpy)_2]$, **2**, may show a signal in the EPR spectrum due to the presence of one Mn^{II} in the molecule. Therefore, the X-band EPR spectra of the two complexes were recorded in a powdered sample at 77 and 4 K and in a CH_2Cl_2/toluene (1:1) glass at 4 K (Figure 7). The spectrum of the solid samples showed a large signal centered at $g \approx 2$, which was slightly split. The intensity of this signal fell with decreasing temperature, and another signal appeared at $g \approx 5.6$, which became quite intense at 4 K. At this temperature the spectrum of the frozen solution was more resolved; it showed several features with g values of ∼2.0, ∼3.1, ∼5.3, and ∼7.3. No attempts were made to interpret these spectra, since they are complicated because of the possible presence of various low-lying spin states quite close to each other, which may give rise to many transitions. Furthermore, the features observed at low fields indicate that ZFS effects may occur, which may thus complicate the analysis of such spectra even further. These spectra are very similar to those reported for the benzoato analogue.[11]

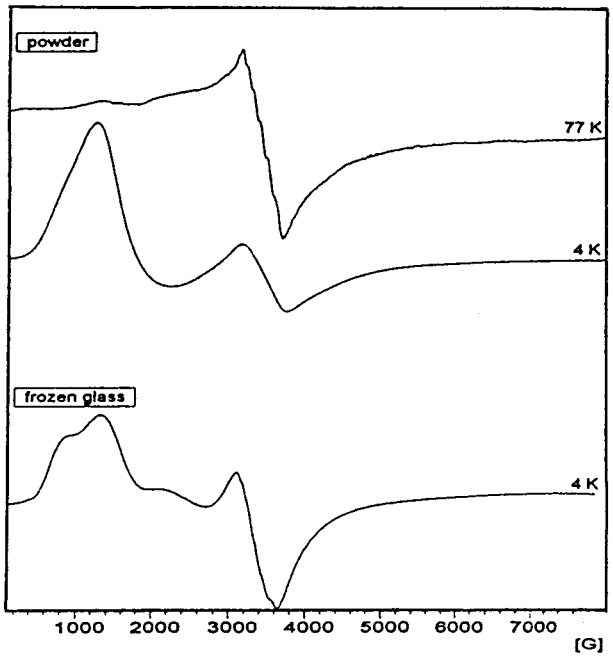

Figure 7. X-band EPR spectra of a powdered sample (top) and a CH_2Cl_2/toluene (1:1) glass (bottom) of $[Mn_4O_2(2\text{-Cl-benzoato})_7(bpy)_2]$ (**1**). The spectra for the 2-Br-benzoato, **2**, are identical.

Acknowledgment. We are very grateful for the financial support given by the Dirección General de Investigación Científica y Técnica (Spain) (Grant PB96/0163) and NATO Project CGR 93/0976. B.A. also aknowledges the F.P.I. Grant from the Ministerio de Educación y Ciencia (Spain). J.R. and M.S.E.F. also acknowledge the help given by the group of Dr. D. Gatteschi (University of Firenze) for the use of the CLUMAG program and acknowledge Dr. Núria Clos for recording the magnetic and EPR data. We thank C. Cañada for the reduced magnetization fit.

Supporting Information Available: X-ray crystallographic file, in CIF format, for **1**. This material is available free of charge via the Internet at http://pubs.acs.org.

IC0010555